Multimode resonance bandpass filter with twin wideband channels

Zhenhua Wang (王振华)*, Yonggang Wu (吴永刚), Zihuan Xia (夏子奂), Renchen Liu (刘仁臣), Gang Lv (吕 刚), Heyun Wu (伍和云), and Pinglin Tang (唐平林)**

Institute of Precision Optical Engineering, Tongji University, Shanghai 200092, China

**Corresponding author: wzh0821@live.cn; **corresponding author: ygwu@tongji.edu.cn*

Received February 14, 2011; accepted March 18, 2011; posted online June 16, 2011;

A bandpass filter with twin wideband channels in a single-layer guided-mode resonance grating is presented. Strong refractive-index modulation is used to support the excitation of multimode resonances $TE_{1,0}$, $TE_{1,1}$, $TE_{2,0}$, $TE_{1,2}$, and $TE_{2,1}$, which are excited by the first and second diffraction orders, relate asymmetrical line shapes and broad low-transmission bands, where TE is the transverse electric. Taking advantage of narrow linewidth and sharp edge line shape in the spectra of $TE_{2,v}$ (v is the mode), a bandpass filter with form factors of 0.61 and 0.7 for long- and short-wave channels is presented to demonstrate this concept.

OCIS codes: 050.1950, 310.2790, 310.6860.

doi: 10.3788/COL201109.080501.

Devices based on guided-mode resonance (GMR) for their application potential have been extensively studied in recent years[1−14]. This GMR mechanism can be applied in constructing a filter that has high diffraction efficiency and narrow linewidth arising from phase matching. Most research to date has addressed the reflection properties of these elements, with the resonance effect providing a high reflection peak or a wide reflection band. Considerably less attention has been paid to resonant bandpass filters that have high transmissivity and wide bandwidth properties. In 2004, Ding *et al.,* presented a narrow bandpass filter based on double resonance in a single-layer periodic waveguide[6,7]. The full-width at half-maximum of the transmission peak was 2.2 nm[6]. Later, Sang *et al.* put forward the concept of resonant enhancement transmission by the overlapping of the edges of multiple leaky mode resonances. The maxima of the twin transmission peaks were all approximately equal to 41%[8].

In this letter, we present a single-layer resonant bandpass filter that has twin wideband channels[15] and very high transmissivity, which are achieved using multimode resonances. The form factors of transmission channels can be modified through asymmetrical line shapes by introducing the modes of high diffraction order to wideband high-reflection spectrum. The form factor (FF) is defined as the ratio of bandwidths between 90% and 50% of maximum transmissivity value, i.e., it is a measure of how well the band approximates an ideal box shape. The closer the ratio is to 1, the closer the passband is to a rectangular shape.

Figure 1 shows the scheme of the proposed single-layer resonant bandpass filter, where $n_{\rm h}$ and $n_{\rm l}$ are the refractive indices of the grating layer, $n_{\rm c}$ and $n_{\rm s}$ are the refractive indices of the air and substrate, respectively, Λ is the grating period, and D is the grating thickness. The numerical method used to calculate the spectra is based on rigorous coupled-wave analysis[16]. For the transverse electric (TE)-polarized normally incident plane wave, the effective index of the periodic waveguide can be approximately estimated by effective medium theory[17], i.e., $n_{\rm eff} = [f n_{\rm h}^2 + (1-f) n_{\rm l}^2]^{1/2}$, where f is the fill factor. The grating modulation is defined as $(n_{\rm h}^2 - n_{\rm l}^2)/(n_{\rm h}^2 + n_{\rm l}^2)$. To achieve resonance, waveguide modes should be generated with the incident wave satisfying the phase-matching condition of the periodic structure, that is

$$\beta_v / k \approx (n_{\rm c} \sin\theta_0 - m\lambda/\Lambda), \tag{1}$$

where β_v is the propagation constant of the mode, k is the propagation constant in free space, and the integer m represents the mth diffracted order. We express the order-mode resonance as $TE_{m,v}$, where v represents the mode.

Using the homogeneous waveguide eigenfunction and relationship expressed in Eq. (1), we plot the mode curves drawn versus wavelength and grating thickness in Fig. 2. For a given normalized filter thickness D/Λ, the locations of the GMR can be read off the plot, which has high reflection peaks. By numerically tuning the parameters such as Λ, D, and $n_{\rm eff}$, we can modify the number of modes and the locations of resonance wavelengths. The modes of $TE_{1,v}$ and $TE_{2,v}$ are both present in the range of $\lambda/\Lambda > 1$, as shown in Fig. 2. That is, the high diffraction order appears at the resonance wavelengths.

The relative permittivity modulation of the periodic waveguide can be expanded into a Fourier series as[6]

$$\varepsilon(x) = \sum_{q=-\infty}^{+\infty} \varepsilon_q \exp(\mathrm{j}qKx), \tag{2}$$

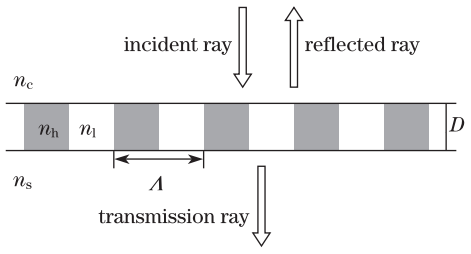

Fig. 1. Scheme of the single-layer sub-wavelength grating under TE illumination.

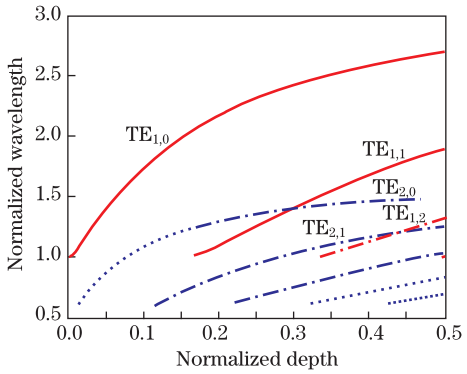

Fig. 2. Estimated resonance locations based on the eigenfunction of the equivalent homogeneous waveguide[6]. Parameters used: n_c=n_s=1 and n_{eff}=3.19.

where ε_q is the qth Fourier harmonic coefficient, and $K = 2\pi/\Lambda$. The grating harmonics $|\varepsilon_q/\varepsilon_0|$ indicate the coupling strength between the qth diffracted order and the incident wave near resonance. The linewidths of the resonances can be controlled by the coupling strength, which is relevant to the grating modulation amplitude. The wide reflection band occurs as a result of the cooperation of several resonance modes excited by the strongly modulated grating. Generally, a larger coupling strength yields a wider linewidth.

Figure 3 shows two Fourier grating harmonics $|\varepsilon_q/\varepsilon_0|$ as a function of fill factor. Because $|\varepsilon_1/\varepsilon_0|$ is always higher than $|\varepsilon_2/\varepsilon_0|$ for a periodic waveguide (the greatest difference between the two is at f=0.5), $TE_{1,\upsilon}$ has wider reflection peaks and can be used to provide the low-transmission background. Considering a numerical example based on Fig. 2 and choosing a suitable parameter for D/Λ, we can select the numbers of modes and introduce those of high diffraction order to the wideband high-reflection spectrum. In this letter, the first and second diffraction orders result in resonance responses with asymmetrical line shapes[2]. We can use these considerations to design the bandpass filter with twin wideband channels and very high transmissivity ($T \approx$100%).

According to Eqs. (1) and (2), when the effective index (n_{eff}=3.19) and fill factor (f=0.5) are kept constant while the refractive indices of the grating layer are altered, we can adjust the grating modulation and the coupling strength depending on the Fourier harmonic coefficient, and then change the resonance linewidths of different modes.

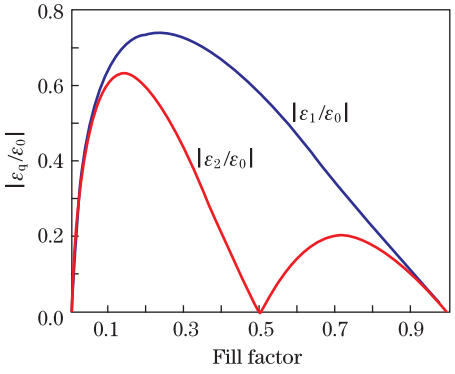

Fig. 3. Fourier grating harmonics $|\varepsilon_q/\varepsilon_0|$ as a function of fill factor[6]. Parameters used: n_h=4.4, n_1=1.

Figure 4 shows the transmittance spectra of the sub-wavelength grating with various modulation strengths at D/Λ =0.39. The locations are indicated clearly in logarithmic scale, seen on the right hand side of the plot in Fig. 4(b). Figure 4(a) shows that the grating modulation increases from 0.12 to 0.23 when n_1 decreases, which results in the expansion of resonance linewidths and the change in resonance locations, i.e., $TE_{1,0}$ shows a blue-shift; $TE_{1,1}$ and $TE_{2,0}$ approach each other; and $TE_{1,2}$ and $TE_{2,1}$ show a red-shift. Using the analysis of Fig. 4(a) as basis, we show the spectra of the bandpass filter with twin wideband channels in the strongly modulated grating in Fig. 4(b). The grating modulation decreases from 0.9 to 0.86 as n_l increases. The leaky mode resonances $TE_{1,1}$ and $TE_{2,0}$ correspond to a wide reflection band; the same is observed for $TE_{1,2}$ and $TE_{2,1}$. The reflectivity is reduced while the overlap of each mode gradually separates. In other words, wideband transmission channels have higher sidebands. Because of the small coupling strength and narrow bandwidth, sharp edge line shapes are detected in the spectra of $TE_{2,\upsilon}$, indicating that the slope of the transmission channel for m=2 is greater than that for m=1, as observed in the short-wave passband shown in Fig. 4(b).

Because of the different coupling strengths (based on Fig. 3), the resonance bandwidth associated with the diffraction orders (m=1, 2) are also varied. To investigate the form factor of the bandpass filter, we modify the mode locations, change the separation of reflectance bands, and take advantage of asymmetric line shapes in the spectra of $TE_{1,\upsilon}$ and $TE_{2,\upsilon}$. When the effective index (n_{eff}=3.19) is kept constant while the D/Λ of the grating layer is altered, we can modify the form factor of the passband.

Figure 5 shows the spectra of the sub-wavelength grating with three different D/Λ values: 0.08, 0.39, and 0.49. As shown in Fig. 5(a) for D/Λ= 0.08, a wide transmission passband with very high transmissivity (T > 99%) arises from the overlap of the edges of leaky mode

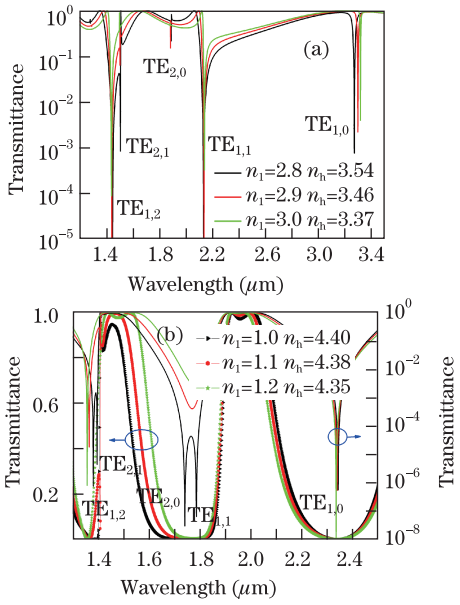

Fig. 4. Spectra of the sub-wavelength grating with different modulation strengths. The parameters used $\Lambda = 1.3\,\mu$m, f=0.5, $D = 0.5\,\mu$m, and n_c=n_s=1.

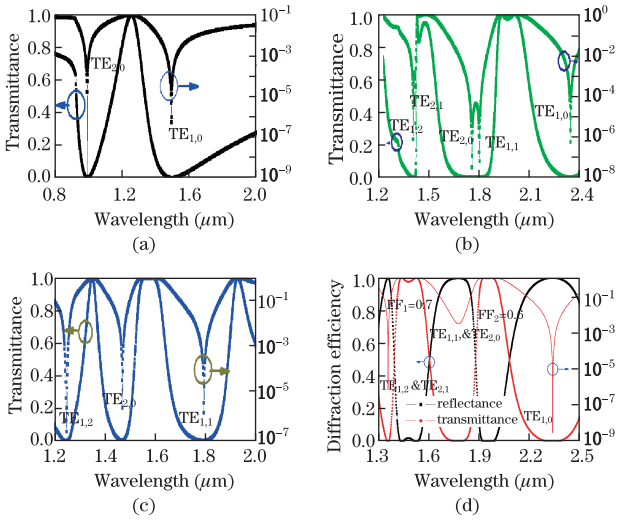

Fig. 5. Transmittance spectra of the sub-wavelength grating with (a) D/Λ=0.08, FF=0.361; (b) D/Λ=0.39, FF_1=0.664, FF_2=0.678; (c) D/Λ=0.49, FF_1=0.348, FF_2=0.638. The parameters used in (d) are: $\Lambda = 1.3\,\mu$m, f=0.5, D=0.5 μm, n_h=4.35, n_1=1.2, and n_h=4.35, n_1=1.2, and n_c=n_s=1.

resonances $TE_{1,0}$ and $TE_{2,0}$. Given the gently sloping transmission sidebands, the form factor is very small (FF=0.361). With the increase in D/Λ to 0.39, the transmittance spectrum changes (Fig. 5(b)). Steep slopes are observed for high-order modes $TE_{1,1}$, $TE_{2,1}$, and $TE_{1,2}$ with asymmetric line shapes and narrow reflection bands. The FFs of short-wave and long-wave passbands improve (FF_1=0.664 and FF_2=0.678, respectively). Figure 5(c) displays the transmission spectra at D/Λ=0.49. More resonance modes and smaller separations are observed between them (compared with those observed in Fig. 2) with FF_1=0.348 and FF_2=0.635. The parameters of the final single-layer filter and the corresponding spectra are shown in Fig. 5(d). The bandwidth of the short-wave channel is 125 nm for $T > 97\%$ (λ=1.425–1.55 μm), whereas that of the long-wave channel is 75 nm for $T > 99\%$ (λ=1.916–1.991 μm). The form factors are FF_1=0.7 and FF_2=0.61, respectively. Of additional interest is that the transmission line shape and the sideband feature are kept almost constant as the grating period is altered while D/Λ is preserved. Thus, we can adjust the passband to the desired wavelength without changing the spectral characteristics.

In conclusion, a twin bandpass filter in a single-layer GMR grating is demonstrated using multiple leaky mode resonances. We design the structure with wide bandwidth channels and very high transmissivity. Through the asymmetrical line shapes and high diffraction efficiency of high-order modes, we investigate the form factor around the designed effective index and D/Λ of the grating layer. The passband can be adjusted to the desired wavelength, with the transmission line shape and the sideband feature almost kept constant by changing the grating period.

This work was supported by the National Natural Science Foundation of China (No. 60977028) and the Key Project Foundation of Shanghai (No. 09JC1413800).

References

1. S. S. Wang and R. Magnusson, Appl. Opt. **32,** 2606 (1993).
2. S. S. Wang and R. Magnusson, Opt. Lett. **19,** 919 (1994).
3. S. Tibuleac and R. Magnusson, J. Opt. Soc. Am. A **14,** 1617 (1997).
4. S. S. Wang and R. Magnusson, Appl. Opt. **34,** 2414 (1995).
5. C. F. R. Mateus, M. C. Y. Huang, Y. Deng, A. R. Neureuther, and C. J. Chang-Hasnain, IEEE Photonics Technol. Lett. **16,** 518 (2004).
6. Y. Ding and R. Magnusson, Opt. Lett. **29,** 1135 (2004).
7. Y. Ding and R. Magnusson, Opt. Express **12,** 5661 (2004).
8. T. Sang, Z. Wang, X. Zhou, and S. Cai, Appl. Phys. Lett. **97,** 071107 (2010).
9. R. Magnusson and S. S. Wang, Appl. Opt. **34,** 8106 (1995).
10. L. Mashev and E. Popov, Opt. Commun. **51,** 131(1984).
11. Z. Wang, T. Sang, J. Zhu, L. Wang, Y. Wu, and L. Chen, Appl. Phys. Lett. **89,** 241119 (2006).
12. Z. Wang, T. Sang, L. Wang, J. Zhu, Y. Wu, and L. Chen, Appl. Phys. Lett. **88,** 251115 (2006).
13. T. Sun, J. Ma, X. Fu, J. Wang, Y. Jin, J. Shao, and Z. Fan, Chin. Opt. Lett. **8,** 447 (2010).
14. X. Fu, K. Yi, J. Shao, and Z. Fan, Chin. Opt. Lett. **7,** 462 (2009).
15. Y. Chen and Z. Wang, Acta Opt. Sin. (in Chinese) **30,** 3064 (2010).
16. T. K. Gaylord and M. G. Moharam, in *Proceedings of IEEE* **73,** 894 (1985).
17. S. M. Rytov, Sov. Phys. JETP **2,** 466 (1956).